INTERNATIONAL
**Agrophysics**
www.international-agrophysics.org

*Int. Agrophys., 2022, 36, 285-295*
doi: 10.31545/intagr/152675

# A semi-empirical equation to predict filling wall pressures on oblique conical hoppers**

*Eutiquio Gallego, José María Fuentes, and Francisco Ayuga**

Buildings, Infrastructures and Projects for Rural and Environmental Engineering (BIPREE), ETSIAAB, Universidad Politécnica de Madrid, 28040 Madrid, Spain

*Received May 10, 2022; accepted August 8, 2022*

A b s t r a c t. Hoppers are frequently used in steel silos, especially in farm facilities and food industries. These structures occasionally have an oblique hopper with an eccentric outlet to improve the flow of material during discharge. The 2006 version of the European standard EN 1991-4 uses classical Walker theory to predict wall pressures on concentric hoppers, but oblique hoppers are not considered. The authors have developed a Finite Element Model to predict the wall pressures on oblique hoppers and several sensitivity analyses have been made to study the possible influence of different parameters including outlet eccentricity, the outlet circumferential position, the aspect ratio of the silo and hopper, and different stored materials. The results show that the circumferential location and eccentricity of the outlet are the main factors affecting the pressures on oblique hoppers. A semi-empirical equation is proposed to estimate the expected pressures on oblique hoppers which is designed to match with the maximum normal pressure obtained from the simulation, and to provide a good representation for the circumferential distribution of normal pressures. The results of this research may be of interest with regard to the upcoming revised version of the European standard EN 1991-4.

K e y w o r d s: Finite Element Method, granular materials, oblique hoppers, wall pressures, steel silos

*Corresponding authors e-mail: francisco.ayuga@upm.es
**This work was supported by the Spanish Agencia Estatal de Investigación via the research project "Study of the structural behaviour of corrugated wall silos using Discrete Element Models (SILODEM)" [grant number PID2019-107051GB-I00/AEI/10.13039/501100011033], (2020-2023).

## INTRODUCTION

Commercial silos are occasionally designed with an oblique hopper in order to facilitate the flow of the bulk solid stored during the discharge process. The term 'oblique hopper' refers to those hoppers where the outlet centroid is not aligned with that of the bin part of the silo. The distribution of normal pressures exerted by a static bulk granular solid on the walls of a concentric conical hopper is well known in the field of silo design and it has already been included in the European Standard concerning silos and tanks EN 1991-4 (2006) under both filling and discharge conditions.

The derivation of the equations included in the current version of EN 1991-4 is considered to have been first developed by Dąbrowski (1957), though it is commonly attributed to Walker (1966). However, EN 1991-4 (2006) does not provide adequate guidance or equations in its current form with which to calculate the pressures exerted by the bulk solid on the inner surface of the wall of oblique hoppers, despite the fact that some numerical analyses have predicted the existence of asymmetrical patterns of pressures in such hoppers for filling conditions (Ayuga *et al*., 2001; Guaita *et al*., 2003; Vidal *et al*., 2006b). Besides, these pressure asymmetries have been reported for discharge condition by Ramirez *et al*. (2010) in silos having oblique hoppers.

Many experimental tests have been conducted to determine the pressures produced by the stored material against the silo walls in bins (Do Nascimento *et al*., 2013; Couto *et al*., 2012; Molenda *et al*., 2009; Brown *et al*., 2000). However, fewer research studies refer to the measurement of wall pressures on hoppers for filling, and all of them consider a centric outlet (Ding *et al.*, 2014; Ramirez *et al*., 2010; Munch-Andersen *et al*., 1992; Aoki and Tsunakawa, 1969). Aoki and Tsunakawa (1969) measured normal wall pressures for concentric steep hoppers using dry silica as a testing material. A small model hopper was considered in this research, and it was found that wall pressures measured for the filling condition agreed with the theoretical values predicted by Walker (1966). Ramirez *et al*. (2010) conducted several tests on three large scale silos employing wheat and maize as testing materials. The cylindrical part of the silo had an aspect ratio of 2.63 (height 5.0 m and diameter 1.9 m), while the height of the hoppers was 1.9 m and the diameter of its circular outlet was 0.32 m. In addition, three different outlet eccentricities were considered: 0, 50 and 100%.

Ramirez *et al*. (2010) compared the normal wall pressures under eccentric outlets with the corresponding values for the concentric case during the filling and discharge processes. During the discharge process, it was found that higher than normal wall pressures were obtained for the wall location opposite to the outlet, while lower pressures occurred at the wall location closer to the outlet. However, for the filling condition with wheat it was found that the higher the hopper eccentricity, the higher the load observed at the transition on the location nearest to the eccentric outlet. Filling pressures with maize were more uniformly distributed around the silo wall. Ramirez *et al*. (2010) theorized that the pattern of the observed filling pressures might be influenced by the inclination of the tube used for filling the silo, which could lead to an eccentric filling.

Ding *et al*. (2014) constructed a shallow concentric hopper of 2.52 m in diameter, 1.21 m in height and with a 0.1 mm outlet diameter to measure normal pressures and friction coefficients at 4 different height levels. The measured normal wall pressures at the end of filling process were significantly higher than those predicted by Walker theory (1966), because in shallow hoppers with a large apex half angle the wall friction is not fully mobilized. On the other hand, the normal wall pressures predicted by the Rotter (2001) theory for shallow hoppers were very close to the experimental values measured. Rotter (2001) proposed the consideration of the same mechanics for shallow hoppers as those suggested by Walker (1966) but adopting an effective hopper wall friction coefficient that would reflect a wall friction that is not fully mobilized.

Some analytical approaches have been proposed to determine the wall pressures on oblique hoppers. Michalowski (1983) derived a formulation to calculate the normal pressures for wedged oblique hoppers, with regard to different wall inclinations. The method developed by the author requires a knowledge of the distribution of the normal stress along the differential slice where the equilibrium is set. However, as a plane stress condition was assumed, the change in the angle of inclination of the hopper wall along the circumferential axis could not be considered. Matchett *et al*. (2009) also proposed a formulation for stress distribution within the bulk solid for wedged oblique hoppers, with a principal stress orientation that follows a circular arc, thereby allowing the backward numerical integration of the force balance equations, and enabling surface and wall boundary conditions to be modelled. The formulation considers different wall inclinations for left and right walls, but again a plane stress condition is assumed.

Many numerical models have been developed to analyse the behaviour of bulk solids stored in concentric hoppers. Finite element (FE) models are used to consider the existence of hoppers in order to obtain the pressures on the walls produced by the stored material (Rotter *et al*., 2019; Kibar, 2017; Wang *et al*., 2013; Ding *et al*., 2011), predict the discharge rate of the material (Zheng *et al*., 2017), wall stresses (Kibar and Ozturk, 2014) or flow characteristics during emptying (Zheng and Yu, 2015). More recently, the Discrete Element technique has been used to characterize the flow (Zhang *et al*., 2018), discharge rate (Kumar *et al*., 2018) or particle segregation of materials stored in hoppers (Xiao *et al*., 2019). However, none of these numerical works considers the existence of oblique hoppers.

Ayuga *et al*. (2001) and Guaita *et al*. (2003) developed Finite element models to study the possible effects of eccentricity on the filling pressures of oblique hoppers. The numerical results obtained in these studies concluded that higher wall pressures would appear at wall locations opposite to the outlet than those corresponding to the concentric case, while a reduction in wall pressures was detected close to the outlet. In addition, the higher the outlet eccentricity, the higher the discrepancy with the concentric case which was found for both opposite wall locations.

Guaita *et al*. (2003) showed that normal pressures on oblique hoppers with full eccentricity tend to follow Janssen´s distribution even for the hopper, and only a progressive decrease in normal pressures was detected because of the silo radius decrease in the hopper. Vidal *et al*. (2008, 2006a) also corroborated these observations for bin-hopper silos, where the real supporting elements were simulated, thereby confirming that the value of the membrane and stress resultants between the supporting columns was also affected by the outlet eccentricity. However, these FE models did not analyse the possible influence of the hopper aspect ratio, silo dimensions or different stored materials in the pressure values.

Therefore, at present, none of the analytical methods proposed in the literature can be directly applied to conical oblique hoppers. Furthermore, the few available results obtained in numerical models (Guaita *et al*., 2003; Ayuga *et al*., 2001) or the experimental tests conducted (Ramirez *et al*., 2010) do not allow for the generalization of any formulation or procedure to estimate the wall pressures on oblique hoppers.

The research work presented in this paper aims to formulate a design equation that would consider the main parameters affecting the calculation of normal pressures on oblique hoppers, *e.g.*, the hopper aspect ratio, bin aspect ratio, hopper eccentricity, wall friction coefficient, wall circumferential location and the material stored in the silo. To this end, a finite element model was developed to calculate the expected normal pressures on oblique hoppers for the different cases analysed.

## MATERIALS AND METHODS

The normal pressures acting on the walls of a conical hopper with a centric outlet (Eq. (1)) taking symmetric filling conditions into account, $p_{nf}$, are included in EN 1991-4 (2006) by using Walker theory (Rotter, 2009), and also includes the changes proposed by Rotter (2001) for shallow hoppers. An effective hopper wall friction coefficient is used for shallow hoppers because wall friction is not fully mobilized:

$$p_{nf} = F_f \; p_{vf} \; . \tag{1}$$

For filling conditions, the value of $F_f$ may be obtained according to Eq. (2), where $\mu_h$ is the wall friction coefficient for the hopper, $\beta$ is the hopper apex half angle, and a is an empirical constant (a=0.8 for filling). For shallow hoppers, the effective or mobilized coefficient of wall friction, $\mu_{heff}$, is used instead of $\mu_h$, and it may be obtained according to Eq. (3), through the lateral pressure ratio ($K$), and the hopper apex half angle ($\beta$):

$$F_f = \frac{1 + a\mu_h \cot\beta}{1 + \mu_h \cot\beta} \; , \tag{2}$$

$$\mu_{heff} = \frac{(1-K)}{2\tan\beta} \; . \tag{3}$$

The value for the mean vertical filling stress in the bulk solid, $p_{vf}$, acting at vertical coordinate x which is defined as positive upwards from the hopper apex is given by Eq. (4), where $\gamma$ is the specific weight of the stored material, $p_{vft}$ is the mean vertical stress acting at the location of the bin-hopper transition, $h_h$ is the vertical height between the hopper apex and the transition, and the exponent, n, is calculated by using Eq. (5):

$$p_{vf} = \frac{\gamma h_h}{n-1}\left\{\left(\frac{x}{h_h}\right) - \left(\frac{x}{h_h}\right)^n\right\} + p_{vft}\left(\frac{x}{h_h}\right)^n \; , \tag{4}$$

$$n = 2\left(F_f \; \mu_h \cot\beta + F_f - 1\right) \; . \tag{5}$$

An FE model was developed with ANSYS (2012) commercial finite element software by assuming the existence of rigid wall filling conditions. The elements used were eight-node isoparametric 3D cubic elements (SOLID45) used to represent the grain, which has plasticity, stress stiffening, a large degree of deflection, and relatively high strain capabilities. The interaction between the stored material and the silo wall was simulated by using a surface contact representation via TARGE170 and CONTA173 elements, and the friction mechanism was assumed to follow Coulomb´s theory. A detailed description of the procedure may be found in Gallego *et al*. (2010).

An elastoplastic constitutive model was used to simulate the behaviour of the material. A classic linear-elastic relationship was used for the elastic part, while the yield criterion of Drucker and Prager (1952) was considered for the plastic part. The mechanical parameters required to simulate the elastic region are Poisson´s ratio ($\nu$), and the modulus of elasticity ($E$). The value for Poisson´s ratio was deduced (Eq. (6)) from the lateral pressure ratio ($K$), defined in EN 1991-4 to facilitate a comparison of the numerical results with Eurocode predictions.

On the other hand, the values for the modulus of elasticity were calculated according to Eq. (7), where $E_{sU}(z)$ is the effective unloading elastic modulus of the stored solid at depth $z$ (as measured from the top of the bin section), $E_{sUo}$ is the initial unloading effective modulus, $\chi_U$ is the unloading modulus contiguity coefficient and $p_{vf}(z)$ is the vertical pressure at depth $z$:

$$\nu = \frac{K}{1+K} \; , \tag{6}$$

$$E_{sU}(z) = E_{sUo} + \chi_U \; p_{vf}(z) \; . \tag{7}$$

The values for the modulus of elasticity adopted for each material and model were deduced from the parameters included in Table 1 (originating from internal experimental tests that were not published), and the vertical pressure existing at the location of the bin-hopper transition, calculated according to EN 1991-4 (2006). The behaviour of the material is completely elastic during the unloading stage, this is the reason why the values used for the parameters required were adopted from this part of the test. The values of the angle of internal friction ($\phi$), were adopted from EN 1991-4 (2006), while the values for cohesion (c), and the angle of dilatancy ($\psi$), were selected from the literature (Couto *et al*., 2013; Moya *et al*., 2013; Moya *et al*., 2002).

**Table 1.** Mechanical parameters considered for stored materials

| Parameter | Wheat | Sugar | Iron Ore Pellets |
|---|---|---|---|
| Specific weight ($\gamma$, kN m$^{-3}$) | 9.0 | 9.5 | 22 |
| Initial unloading effective modulus of elasticity ($E_{sUo}$, kPa) | 4700 | 1730 | 1500 |
| Unloading modulus contiguity coefficient ($\chi_U$) | 100 | 390 | 480 |
| Lateral pressure ratio ($K$) | 0.54 | 0.5 | 0.54 |
| Poisson's ratio ($\nu$) | 0.35 | 0.33 | 0.34 |
| Angle of internal friction ($\phi$, °) | 30 | 32 | 31 |
| Cohesion (c, kPa) | 2 | 0 | 0 |
| Dilatancy angle ($\psi$, °) | 10 | 0 | 10 |
| Grain-to-wall friction coefficient ($\mu$) | 0.38 | 0.46 | 0.49 |

A bin-hopper geometry was adopted to simulate the silo (Fig. 1a), while the geometry of an oblique hopper was developed according to the plan view as defined in Fig. 1b, where $\theta$ denotes the circumferential position for the oblique hopper wall considered, with the origin ($\theta$=0º) at the wall location closest to the eccentric outlet. The dimensions of the different parameters used to construct the silo geometry may be found in Table 2.

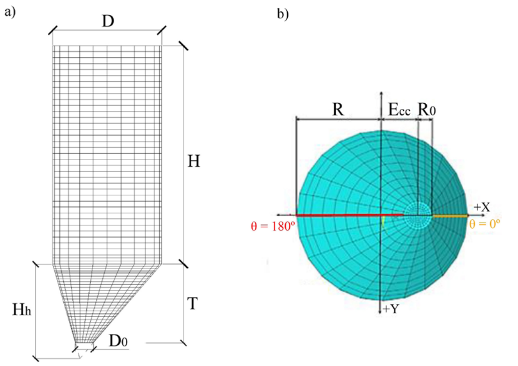


**Fig. 1.** Geometry of the simulated silo; a) dimensions of bin and hopper; b) parameters defining silo hopper.

Table 2 also shows the different values considered for sensitivity analyses. The values adopted for the aspect ratio of the bin section (H/D) are those most widely used in commercial silos. For the same reason, the different values employed for the oblique hopper aspect ratio ($H_h$/D) are those typically used by silo manufacturers. The angle of inclination of a concentric cylindrical hopper with respect to the horizontal axis usually ranges between 45 and 60º to facilitate material flow during discharge. Thus, the corresponding oblique hopper aspect ratios ($H_h$/D) would be 0.5 and 0.86 respectively. However, two additional hopper aspect ratios of 0.63 and 1.2 have also been considered (corresponding to angles of inclination 51 and 68º) in order to investigate the possible influence of this parameter.

**Table 2.** Dimensions considered for geometrical parameters

| Parameter | Dimensions |
|---|---|
| D: diameter of silo | 6 m |
| R: radius of silo | 3 m |
| $D_o$: diameter of outlet | 1 m |
| $R_o$: radius of outlet | 0.5 m |
| H: vertical height of bin section | 6-12-18 m |
| T: vertical height of hopper section | 6.25-4.33-3.125-2.5 m |
| (H/D) Aspect ratio for the bin section | 1-2-3 |
| ($H_h$/D) Aspect ratio for the oblique hopper | 0.5-0.63-0.86-1.25 |
| $E_{cc}$: Outlet eccentricity of the oblique hopper | 0-0.625-1.25-1.875-2.5 m |

## RESULTS

The outlet eccentricity ratio ($e_0$), may be obtained from the outlet eccentricity of the hopper and the diameters of the bin and hopper sections of the silo (Eq. (8)). In order to allow for a comparison to be made between the FE results corresponding to the different hopper aspect ratios, (R/$H_h$), dimensionless hopper heights ($\overline{Z}$), have been obtained (Eq. (9)), by normalising the vertical height between the hopper apex and the hopper location ($Z_h$), by using the vertical height between the hopper apex and the hopper top ($H_h$):

$$e_0 = \left(\frac{2E_{cc}}{D - D_o}\right), \tag{8}$$

$$\overline{Z} = \left(\frac{Z_h}{H_h}\right). \tag{9}$$

In addition, in all cases a coefficient ($C_{oh,f}$) has been obtained corresponding to the oblique hopper analysed for filling (Eq. (10)), where the normal pressures predicted by the FE model ($p_n$), are divided by the normal pressures obtained according to the Eurocode standard ($p_{n,EN}$), for a silo with a concentric hopper.

$$C_{oh,f} = \left(\frac{p_n}{p_{n,EN}}\right). \tag{10}$$

Fig. 2 shows the normal wall pressures calculated for a silo with an aspect ratio (H/D=2) for the bin, 60º for the oblique hopper ($H_h$/D=0.86) and considering wheat as the stored material. It may be checked if the normal pressures predicted by the FE model match the values provided by EN 1991-4 (2006) for the bin section, while they are slightly lower for the hopper assuming a concentric case ($e_0$=0).

The FE results further illustrate that the normal wall pressures increase with the oblique hopper eccentricity for the wall location opposite to the outlet (circumferential position $\theta$=180º), while a decrease is detected for the wall location closer to the outlet (circumferential position

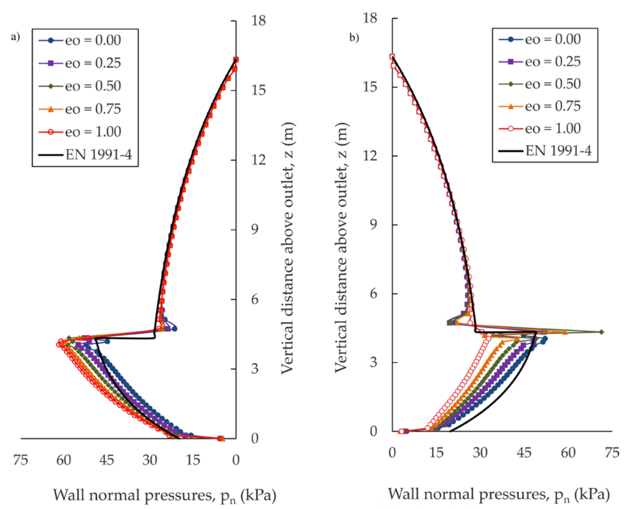


**Fig. 2.** Wall normal pressures obtained for wheat, considering different outlet eccentricities, $e_0$, and circumferential positions $\theta$; a) $\theta$=180º, b) $\theta$=0º.

$\theta$=0º). This trend was obtained for all of the different cases and materials considered, and it matches with the results obtained by Guaita *et al*. (2003) and Ayuga *et al*. (2001). Because of the close agreement between the FE results and the EN 1991-4 predictions, the results for the bin section of the silo will be omitted in the following sections, and only the calculations for the hopper section will be included.

It is also important to note that the normal pressures predicted for the oblique hopper case ($e_0$=1) exactly match those corresponding to the concentric outlet ($e_0$=0) at the circumferential locations $\theta$=90º and $\theta$=270º (Fig. 3). Because of this, the normal wall pressures will be checked in sections 3.1 to 3.3 only for the circumferential locations exhibiting extreme values ($\theta$=0º and $\theta$=180º).

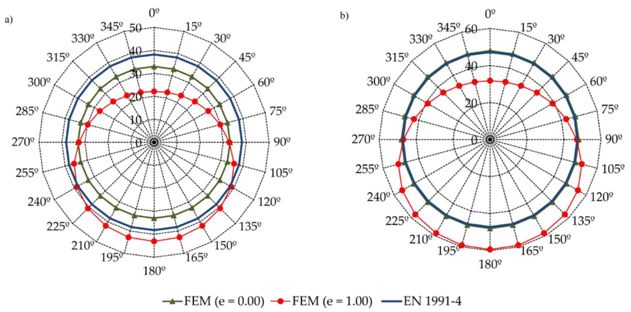


**Fig. 3.** Comparison of wall normal pressures ($p_n$, kPa) along the circumferential position between Finite Element Model (FEM) predictions and Eurocode (EN 1991–4), for wheat at different hopper dimensionless heights; a) $\overline{Z}$=0.5, b) $\overline{Z}$=0.9.

Fig. 3 shows the circumferential distribution of normal wall pressures obtained with FE for both extreme oblique hopper cases ($e_0$=0 and $e_0$=1), and the predictions corresponding to EN 1991-4 at two different hopper heights. It may be seen that there is a good agreement between the numerical results and the Eurocode predictions for the concentric case ($e_0$=0): at $\overline{Z}$=0.5, the FE results predict a normal wall pressure of 33 kPa, while EN 1991-4 predicts 38 kPa, and a very close match was obtained at $\overline{Z}$=0.9. A similar trend can also be observed for other $\overline{Z}$ values.

The increase in outlet eccentricity causes the hopper wall closer to the outlet ($\theta$=0º) to be steeper, thus reducing the weight of the material transferred to the wall. This effect leads to a decrease in the normal wall pressures with regard to the concentric case. For maximum eccentricity ($e_0$=1), the hopper wall would be a prolongation of the bin wall, then the normal wall pressures observed tend to follow Janssens distribution, but with some lower values because of the decrease in the silo radius when approaching the outlet. On the other hand, the opposite effect may be observed for the opposite wall ($\theta$=180º). If outlet eccentricity increases, the wall opposite to the outlet becomes shallower, and therefore a higher weight of stored material must be supported by the hopper wall, thereby leading to greater normal pressures.

According to EN 1991-4, hoppers may be classified as steep or shallow, depending on several parameters. The hopper aspect ratio, $H_h/D$, affects the steepness of the hopper, and it is one of the parameters that can change the fundamental characteristics of the hopper. Friction is not fully mobilised for shallow hoppers (Rotter, 2001), which changes the distribution of normal pressures applied to the wall hoppers. With wheat as the stored material, a bin aspect ratio of H/D=2.0 was considered in this section to remove any possible influence of other parameters in the sensitivity analyses of $H_h/D$.

Fig. 4 shows the change in the coefficient of pressures for the oblique hopper ($C_{oh,f}$), with respect to the hopper dimensionless height ($\overline{Z}$), and the values of $H_h/D$ considered for different outlet eccentricities ($e_0$=0, $e_0$=0.5 and $e_0$=1) and both extreme wall circumferential locations ($\theta$=0º and $\theta$=180º). It has been observed for all of the cases analysed that $C_{oh,f}$ decreases from its maximum value (located at the bin-hopper transition) to its minimum value at the hopper outlet following an approximately a linear trend.

The coefficient of pressures obtained at the oblique hopper wall closer to the outlet (Fig. 4a-4c) is not significantly affected by the change in $H_h/D$, especially for low outlet eccentricities ($e_0$=0 and $e_0$=0.5). The values obtained for $C_{oh,f}$ when $\overline{Z}$ is in the range of 0.25 to 0.9 for the different cases studied are quite close, and only maximum differences of up to 25% between the extreme cases analysed may be observed for the full oblique hopper eccentricity ($e_0$=1). $C_{oh,f}$ varies between 0.8 and 1.2 for the concentric case ($e_0$=0) and at hopper dimensionless height intervals of 0.25-0.9, while a progressive decrease in the pressure coefficient is detected when the oblique hopper eccentricity increases.

The bin-hopper transition produces an abrupt change in geometry, which usually leads to some numerical effects that can slightly distort the results obtained (Keiter and Rombach, 2001) when a Finite Element model is developed. In addition, all displacements were restrained for those nodes placed at the outlet to simulate filling conditions. Because of these factors, some slight differences for $C_{oh,f}$ may be found at both hopper endings: outlet ($\overline{Z}$ interval 0.17-0.25) and bin – hopper transition ($\overline{Z}$ interval 0.9-1), but they are not significant and should not be considered during the analyses because of the singularities described.

Fig. 4d-4f shows the results obtained for the oblique hopper wall opposite to the outlet ($\theta$=180º). As expected, the results for the concentric case ($e_0$=0) are the same as those previously calculated for ($\theta$=0º). It has also been checked if $C_{oh,f}$ is greater than 1 for eccentric oblique hoppers ($e_0$>0). Again, the bin-hopper transition singularity affects the value of $C_{oh,f}$ for the $\overline{Z}$ interval 0.9-1, while their values remain almost stable up to $\overline{Z}$=0.5, with no significant differences found among the different $H_h/D$ values.

The values for $C_{oh,f}$ obtained at specific $\overline{Z}$ locations to calculate the $H_h/D$ values were considered to have been represented by (Figs 5 and 6) in order to find possible trends

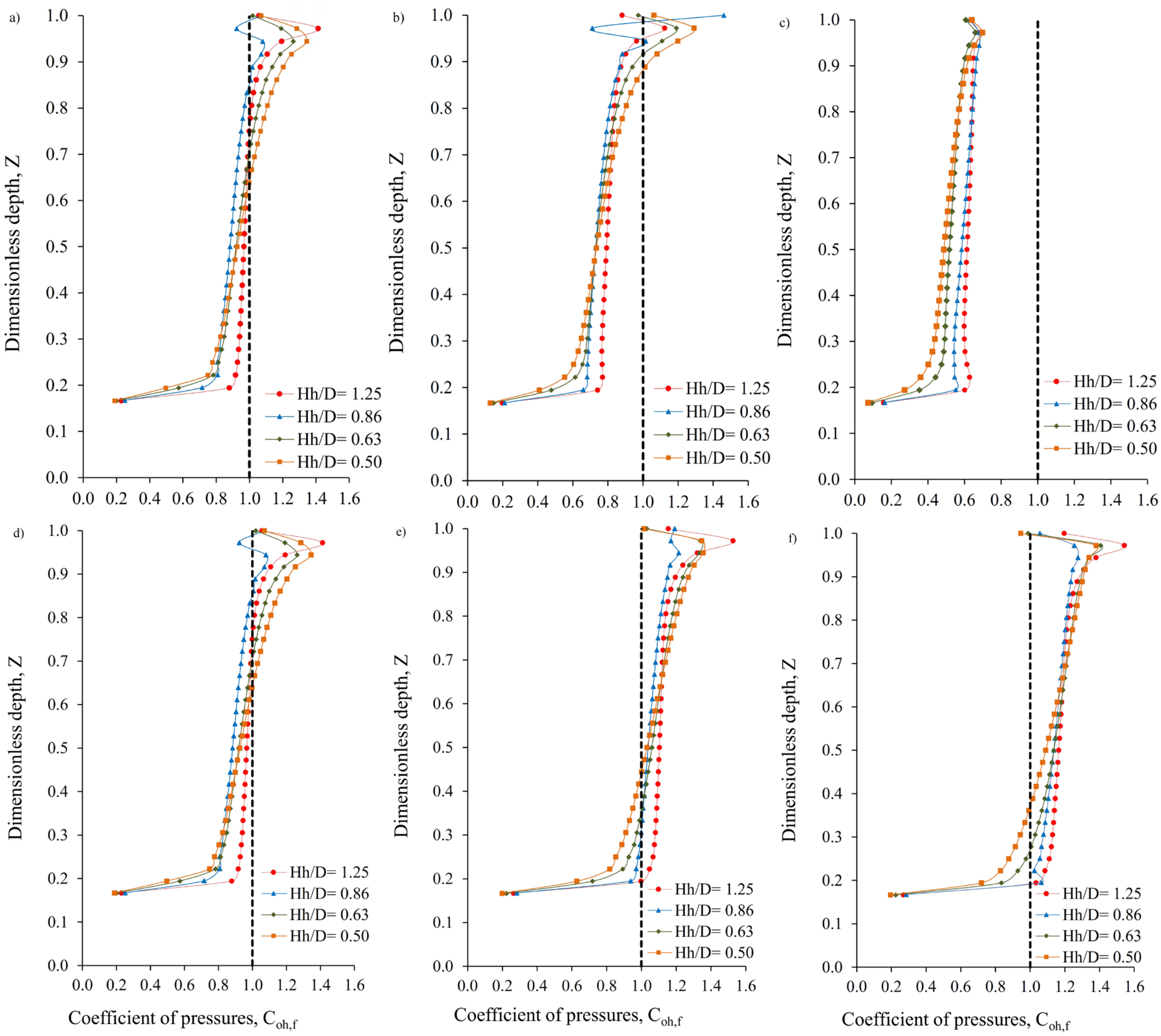


**Fig. 4.** Coefficient of pressures obtained for the oblique hopper in a silo with a bin aspect ratio H/D=2.0, and wheat as stored material; a) $\theta$=0º, $e_0$=0; b) $\theta$=0º, $e_0$=0.5; c) $\theta$=0º, $e_0$=1; d) $\theta$=180º, $e_0$=0; e) $\theta$=180º, $e_0$=0.5; f) $\theta$=180º, $e_0$=1.

more clearly. The values of $C_{oh,f}$ obtained for the concentric case ($e_0$=0) are very close to 1 for any height $\bar{Z}$ and circumferential position, thus indicating that FE models predict the same normal pressures as those in Eurocode EN 1991-4. The results obtained at the circumferential locations $\theta$=180º (Fig. 5) and $\theta$=0º (Fig. 6) show that $H_h$/D does not affect $C_{oh,f}$ for most locations of the hopper wall, while taking into account the independence of the outlet eccentricity.

The maximum differences between the different $H_h$/D cases analysed are found at $\bar{Z}$=0.25, where a 30% difference in $C_{oh,f}$ appears for the extreme cases of $H_h$/D considered. However, this height is very close to the hopper outlet, where normal wall pressures are significantly lower than those obtained at locations closer to the bin-hopper transition. The differences found in $C_{oh,f}$ values at locations closer to the transition ($\bar{Z}$>0.75), where peak normal pressures appear on the hopper, are always lower than 20% for any $H_h$/D value simulated.

The increase in the bin aspect ratio, H/D, implies an increase in mean vertical stress in the solid at the bin-hopper transition. This pressure value is used to obtain the distribution of vertical and normal pressures on the hopper walls. In addition, the increase in the vertical pressures at the transition may lead to a higher degree of confinement of the stored material which may in turn influence the mobilization of the material and, therefore, the pattern of normal pressures obtained at the hopper. Three different H/D values were used (1, 2 and 3) in the analysis. The hopper aspect ratio $H_h$/D does not seem to significantly affect the normal pressures on the oblique hoppers for any outlet eccentricity, as concluded in the previous section. Thus, the

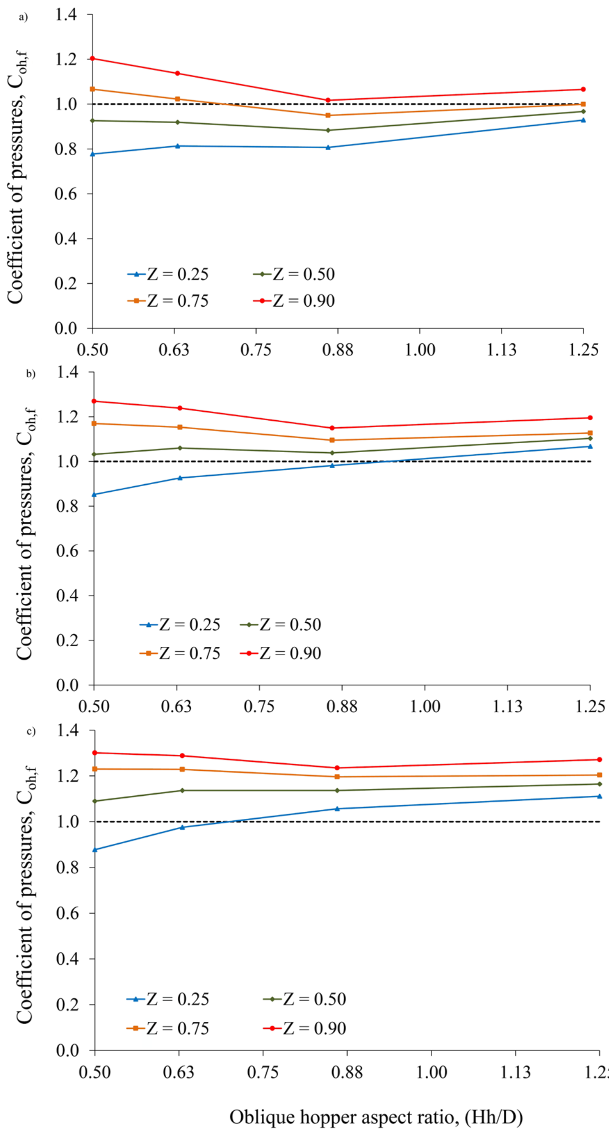


**Fig. 5.** Coefficient of pressures obtained for the oblique hopper in a silo with bin aspect ratio H/D=2.0 at different hopper dimensionless heights, $\overline{Z}$, for circumferential location $\theta$=180º and varying the outlet eccentricity; a) $e_0$=0, b) $e_0$=0.5, c) $e_0$=1.

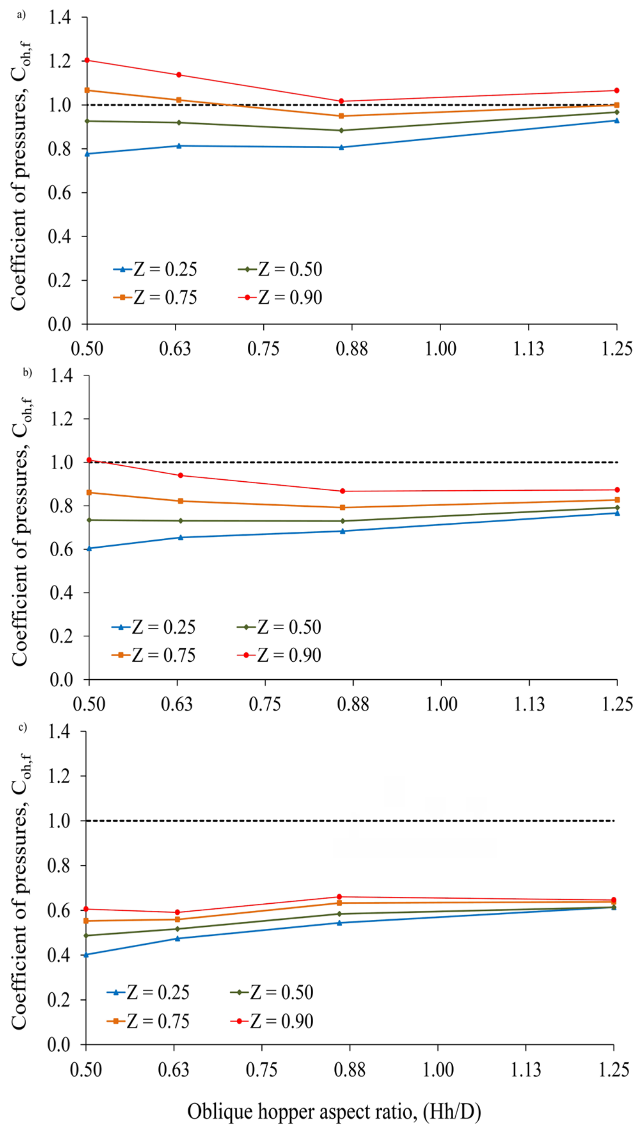


**Fig. 6.** Coefficient of pressures obtained for the oblique hopper in a silo with bin aspect ratio H/D=2.0 at different hopper dimensionless heights, $\overline{Z}$, for circumferential location $\theta$=0º and varying the outlet eccentricity; a) $e_0$=0, b) $e_0$=0.5, c) $e_0$=1.

value $H_h$/D=0.86 has been adopted in all cases because it corresponds to the most frequently used hopper in industrial silos (60º angle of inclination).

The increase in mean vertical stress also implies a change in the modulus of elasticity of the material (Eq. (6)). This is the reason why this section includes analyses concerning the possible influence of the modulus of elasticity of the material on the pattern of normal pressures obtained from oblique hoppers. An elastoplastic criterion has been considered for the material stored in the silo. Thus, a different modulus of elasticity can lead to differences in the behaviour of the material stored. For example, an increase in the modulus of elasticity leads to an increase in the relative stiffness of the material with regard to the hopper wall, which could eventually lead to changes in the pattern of normal pressures. Table 3 shows the values obtained for the effective modulus of elasticity of the three materials considered for the different H/D ratios used in the FE analyses.

Fig. 7 shows the values obtained for $C_{oh,f}$ at $\overline{Z}$=0.9 for all of the materials considered, both reference circumferential locations and the H/D value were used. The values of H/D are

**Table 3.** Effective modulus of elasticity, $E_{sU}$, used for stored materials in FE models

| Material | $\gamma$ (kN m$^{-3}$) | $E_{sUo}$ (kPa) | $x_U$ | $E_{sU}$ (kPa) H/D=1.0 | H/D=2.0 | H/D=3.0 |
|---|---|---|---|---|---|---|
| Wheat | 9.0 | 4700 | 100 | 8384 | 10674 | 10718 |
| Sugar | 9.5 | 1730 | 390 | 16265 | 22053 | 24365 |
| Iron ore pellets | 22 | 1500 | 480 | 41234 | 55570 | 60746 |

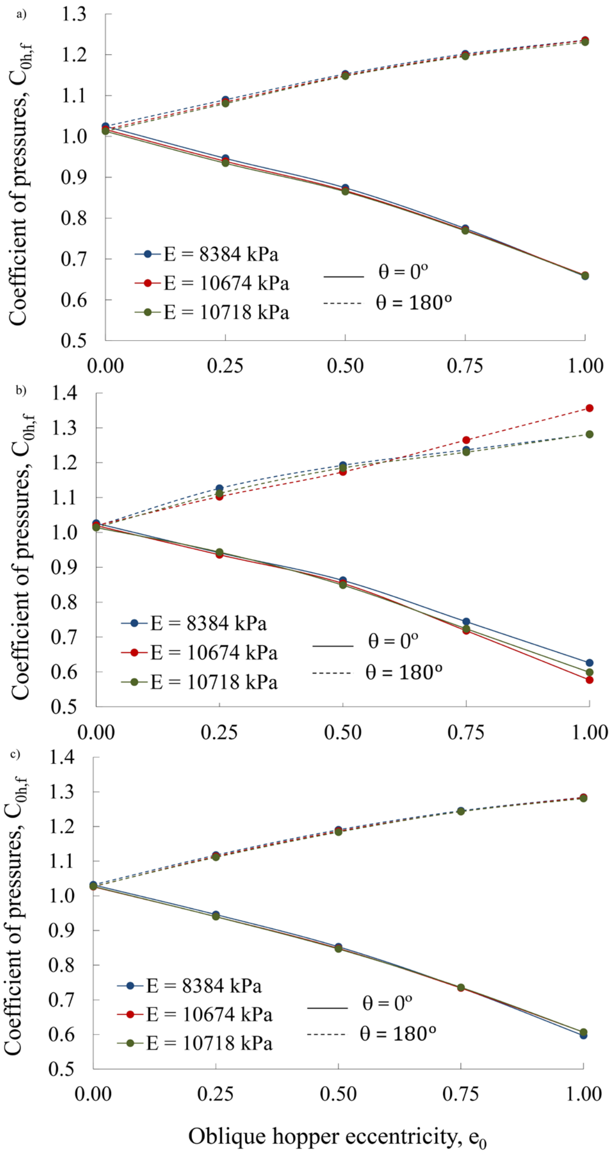


**Fig. 7.** Coefficient of pressures obtained for the oblique hopper in a silo with different bin aspect ratios, (H/D), at circumferential locations $\theta$=0º and 180º; a) wheat, b) sugar, c) iron ore pellets.

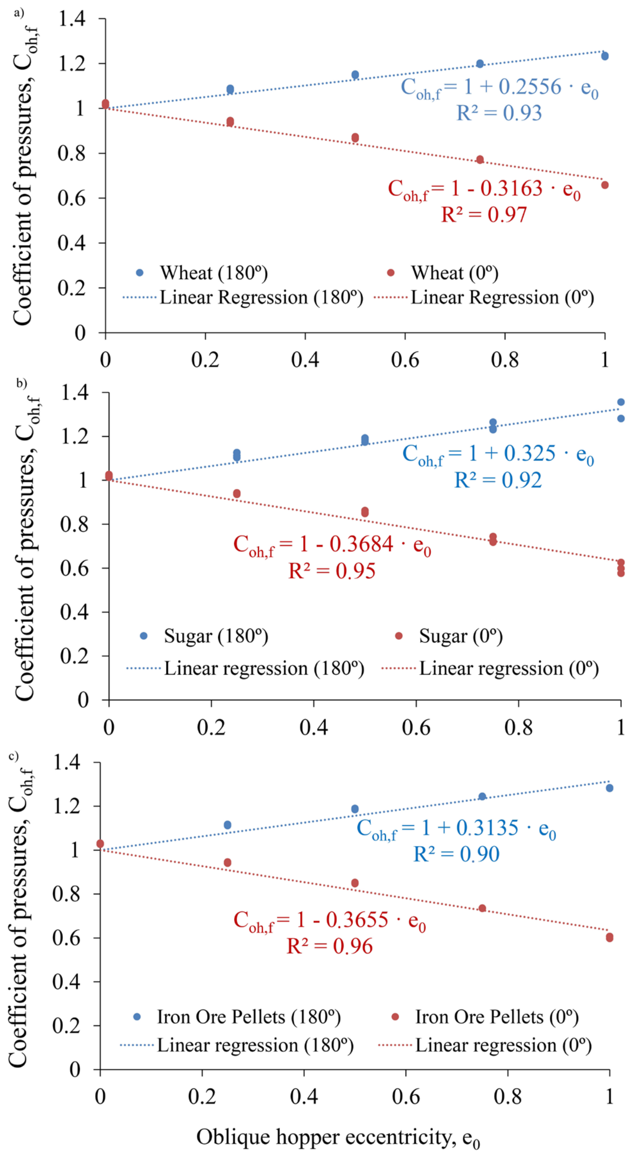


**Fig. 8.** Coefficient of pressures obtained for the oblique hopper as a function of oblique hopper eccentricity; a) wheat, b) sugar, c) iron ore pellets.

**Table 4.** Coefficients of pressure obtained at circumferential location $\theta$=0º and hopper dimensionless height $\overline{Z}$=0.9

| H/D | Material | Oblique Hopper eccentricity ($e_0$) | | | | |
|---|---|---|---|---|---|---|
| | | 0.00 | 0.25 | 0.50 | 0.75 | 1.00 |
| 1.0 | Wheat | 1.02 | 0.95 | 0.87 | 0.77 | 0.66 |
| | Sugar | 1.03 | 0.94 | 0.86 | 0.74 | 0.63 |
| | Iron ore pellets | 1.03 | 0.95 | 0.85 | 0.73 | 0.60 |
| 2.0 | Wheat | 1.02 | 0.94 | 0.87 | 0.77 | 0.66 |
| | Sugar | 1.02 | 0.94 | 0.85 | 0.72 | 0.58 |
| | Iron ore pellets | 1.03 | 0.94 | 0.85 | 0.73 | 0.61 |
| 3.0 | Wheat | 1.01 | 0.93 | 0.86 | 0.77 | 0.66 |
| | Sugar | 1.01 | 0.94 | 0.85 | 0.72 | 0.60 |
| | Iron ore pellets | 1.03 | 0.94 | 0.85 | 0.74 | 0.61 |

**Table 5.** Coefficients of pressure obtained at circumferential location $\theta$=180º and hopper dimensionless height $\overline{Z}$=0.9

| H/D | Material | Oblique Hopper eccentricity ($e_0$) | | | | |
|---|---|---|---|---|---|---|
| | | 0.00 | 0.25 | 0.50 | 0.75 | 1.00 |
| 1.0 | Wheat | 1.02 | 1.09 | 1.15 | 1.20 | 1.24 |
| | Sugar | 1.02 | 1.13 | 1.19 | 1.24 | 1.28 |
| | Iron ore pellets | 1.03 | 1.12 | 1.19 | 1.25 | 1.28 |
| 2.0 | Wheat | 1.02 | 1.08 | 1.15 | 1.20 | 1.24 |
| | Sugar | 1.02 | 1.10 | 1.17 | 1.26 | 1.36 |
| | Iron ore pellets | 1.03 | 1.11 | 1.19 | 1.24 | 1.28 |
| 3.0 | Wheat | 1.01 | 1.08 | 1.15 | 1.20 | 1.23 |
| | Sugar | 1.01 | 1.11 | 1.18 | 1.23 | 1.28 |
| | Iron ore pellets | 1.03 | 1.11 | 1.18 | 1.24 | 1.28 |

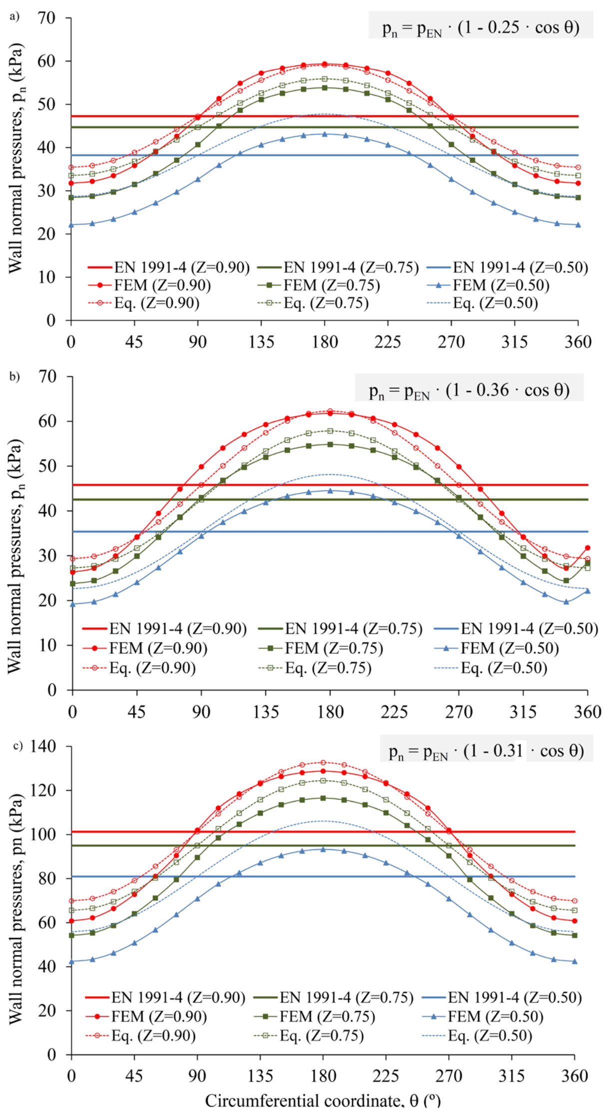


**Fig. 9.** Wall normal pressures along the circumferential coordinate obtained with FE models and predicted by proposed equations for oblique hopper eccentricity $e_0$=1; a) wheat, b) sugar, c) iron ore pellets.

not explicitly considered, because it is the preferred option to represent the effective modulus of elasticity obtained for each material (Table 2). It may be concluded that there is no significant effect produced by the material used, the H/D ratio or the effective modulus of elasticity. In all cases, if the outlet eccentricity and circumferential location are considered, then similar $C_{oh,f}$ values are obtained for all materials independently of the H/D value or modulus of elasticity. The peak value of $C_{oh,f}$ is obtained for $e_0$=1 and $\theta$=180º, and lies in the range 1.26-1.36 in all cases. The minimum value of $C_{oh,f}$ may be observed for $e_0$=1 and $\theta$=0º, and lies in the range 0.6-0.65 independently of the material used or the H/D value considered. The results observed in Fig. 7 are also detected at any other $\overline{Z}$ location.

The numerical results obtained illustrate that the circumferential location and outlet eccentricity are the main factors affecting the local value of the normal wall pressures existing in oblique hoppers. In addition, it has been found that $\overline{Z}$=0.9 provides the most significant value for the coefficient of pressures in oblique hoppers for both of the referenced circumferential locations ($\theta$=0º and 180º).

Tables 4 and 5 show coefficients of pressure $C_{oh,f}$ obtained at a hopper dimensionless height of 0.9 for circumferential locations of 0 and 180º, respectively, and considering different materials and bin aspect ratios. The aspect ratio considered for all hoppers was the same ($H_h/D$=0.86). The influence of the outlet eccentricity is significant, but that of the material was found to be negligible. Also, it is important to check that the coefficient of the pressures obtained is very close to 1 for all materials or bin aspect ratios when a concentric outlet is considered ($e_0$=0). This would mean that the pressures predicted by FE would match the normal pressures as calculated by using EN 1991-4. Therefore, the proposed equation could also be valid for the general case involving a concentric outlet. If all of the results obtained for every simulation and material are represented with respect to the oblique hopper eccentricity (Fig. 8), a linear relationship between the coefficient of pressures and the oblique hopper eccentricity may be observed.

The coefficient of determination $R^2$ is greater than 0.9 for all of the materials considered in the various simulations (Fig. 8), thereby indicating the existence of a very close correlation between the coefficient of pressures and oblique hopper eccentricity.

It can also be checked if the coefficient affecting the oblique hopper eccentricity ranges in the interval of 0.26-0.36 for all cases and circumferential locations, with a positive sign for the circumferential location of $\theta$=180º and a negative sign for the circumferential location of $\theta$=0º.

Therefore, it is proposed that the normal wall pressures in oblique hoppers ($p_{oh,f}(\theta)$), can be calculated at any hopper height and for any circumferential location $\theta$ by multiplying the normal pressure calculated according to the applicable Eurocode for the concentric case ($p_{n,EN}$), and the corresponding coefficient of pressures, $C_{oh,f}$ (Eq.11).

$$p_{oh,f} = C_{oh,f}\,(\theta)\, p_{n,EN}\ . \tag{11}$$

The value for the coefficient of pressures may be calculated using the circumferential location ($\theta$), the oblique hopper eccentricity, $e_0$, and the coefficient obtained for each material, $k$ (Eq. 12).

$$C_{oh,f} = (1 - k\, e_0\, \cos\theta)\ . \tag{12}$$

The proposed equation would also be valid for the calculation of normal pressures on concentric hoppers according to the equations defined in EN 1991-4. In this case, hopper eccentricity would be $e_0$=0, thus leading to a value of $C_{oh,f}$=1 which would generate a uniform normal pressure along the circumferential position.

Fig. 9 shows a comparison between the normal pressures obtained using FE modelling for an oblique hopper with an eccentricity of $e_0$=1 and H/D=2, and the predicted values calculated through Eqs (11-12) for wheat, sugar, and iron ore pellets by considering the values of coefficient $k$ equal to 0.26, 0.36 and 0.31 respectively. A comparison of the results has also been carried out for three hopper dimensionless heights ($\overline{Z}$): 0.9, 0.75 and 0.5.

The normal wall pressures predicted by the proposed equations match the FE observed values very well, especially for hopper wall heights with greater pressures ($\overline{Z}$=0.9 and 0.75). If the results for wheat material and hopper height $\overline{Z}$=0.9 are considered, then the difference between the predicted and the FE values is less than 5% for the circumferential location interval (60-300º), and the maximum difference is only 10% at other circumferential coordinates.

In addition, the difference between both values is only 0.3% for a circumferential coordinate of $\theta$=180º (59.5 kPa *vs* 59.4 kPa), at which point the maximum normal pressures appear. These differences are slightly greater for a dimensionless hopper height equal to 0.75. In this case, the difference between the predicted and the FE value at the circumferential coordinate having a peak normal wall pressure ($\theta$=180º) increases up to 4.7% (56.3 *vs* 53.8 kPa).

The results obtained for sugar (Fig. 9b) also show a very good agreement between the values predicted by the equation proposed and those obtained using the FE models. For example, the difference between both sets of results is only in the range of 0.9 and 5.5% at the dimensionless heights of 0.9 and 0.75, respectively, and at the circumferential coordinate where the peak normal pressure occurs ($\theta$=180º).

The difference between the predicted and numerical values is lower than 10% for the circumferential coordinate interval ranging between 30 and 330º at both dimensionless heights (0.9 and 0.75). The results obtained for iron ore pellets (Fig. 9c) show the same tendency as that observed for sugar or wheat, and only slightly greater differences between the predicted and the numerical values are obtained. For example, the difference between both sets of results is now at 3.0% at the dimensionless height of 0.9 and for the circumferential coordinate where the peak normal pressure occurs ($\theta$=180º).

The equations resulting from the previous analysis have been derived for a limited number of materials and silo geometries. This means that their direct application to a standard for a wider range of materials and geometries could be risky. A magnified value of $k$ in Eq. (12) would be advisable. It is not possible to indicate such a value here, because it depends on other factors and safety coefficients. These may be different for each standard.

## CONCLUSIONS

A finite element model was developed to predict the normal wall pressures on oblique hoppers. This has corroborated previous findings concerning the influence of the circumferential position on normal wall pressures, and the following conclusions were obtained:

1. A decrease in normal pressures on the wall closer to the eccentric outlet was predicted together with an increase of pressures on the opposite wall relative to a concentric hopper. The highest increase of pressures predicted by numerical models was not found to exceed 1.4 times the value predicted by Eurocode EN 1991-4 for the corresponding concentric hopper.

2. The change in pressures with respect to the concentric case remains almost constant for the entire hopper wall, and only a low number of significant differences appear at the top (bin-hopper transition) or bottom (outlet) locations. However, the abrupt changes found at these locations may be explained by the numerical singularities associated with the development of the finite element model.

3. The outlet eccentricity of oblique hoppers also affects the ratio of the increase or decrease in normal wall pressures relative to the concentric hopper. If the outlet eccentricity increases, then the existing overpressure at the hopper wall opposite to the outlet also tends to increase, while the pressures on the wall closer to the outlet tends to decrease.

4. Some parameters do not seem to have any significant influence over the normal pressures on oblique hoppers, such as the bin aspect ratio, the hopper aspect ratio, or the bulk material. No significant relationships have been found between them with respect to changes in the coefficient of pressures obtained for oblique hoppers.

5. An analytical equation was proposed to calculate the normal wall pressures on oblique hoppers, including their circumferential variation. The prediction of peak normal pressures made by the proposed equation differs by less than 3% from the finite element simulations for the cases studied.

## ACKNOWLEDGMENTS

The authors would like to thank Prof. Sadowski for his remarks and useful suggestions and to recognise the suggestions, compromise and support of Prof. Rotter during the entire research conducted.

**Conflict of interest:** All authors declare no conflict of interest.

## REFERENCES

**Ansys, 2012.** ANSYS User's manual. Version 13.0, ANSYS, Canonsburg, PA, USA.

**Aoki R. and Tsunakawa H., 1969.** The pressure in a granular material at the wall of bins and hoppers. J. Chem. Eng. Japan, 2(1), 126-129, https://doi.org/10.1252/jcej.2.126.

**Ayuga F., Guaita M., Aguado P.J., and Couto A., 2001.** Discharge and the eccentricity of the hopper influence on the silo wall pressures. J. Eng. Mech.-ASCE, 127(10), 1067-1074, https://doi.org/10.1061/(ASCE)0733-9399(2001)127:10(1067)

**Brown C.J., Lahlouh E.H., and Rotter J.M., 2000.** Experiments on a square plan form steel silo. Chem. Eng. Sci., 55(20), 4399-4413, https://doi.org/10.1016/S0009-2509(99)00574-6

**Couto A., Ruiz A., and Aguado P.J., 2012.** Design and instrumentation of a mid-size test station for measuring static and dynamic pressures in silos under different conditions - Part I: Description. Comput. Electron. Agric., 85(1), 164-173, https://doi.org/10.1016/j.compag.2012.04.009

**Couto A., Ruiz A., and Aguado P.J., 2013.** Experimental study of the pressures exerted by wheat stored in slender cylindrical silos, varying the flow rate of material during discharge. Comparison with Eurocode 1 part 4. Powder Technol., 237(1), 450-467, https://doi.org/10.1016/j.powtec.2012.12.030

**Dąbrowski A., 1957.** Pressures in bulk solids in hoppers. (In Polish), Arch. Inżynierii Lądowej. 3, 325-334.

**Ding S., Ji Y., Ye S., Rotter J.M., and Li Q., 2014.** Measurements of pressure and frictional tractions along walls of a large-scale conical shallow hopper and comparison with Eurocode 1991-4:2006. Thin-Walled Struct., 80(1), 231-238, https://doi.org/10.1016/j.tws.2014.03.008

**Ding S., Rotter J.M., Ooi J.Y., and Enstad G., 2011.** Development of normal pressure and frictional traction along the walls of a steep conical hopper during filling, Thin-Walled Struct., 49(12), 1246-1250, https://doi.org/10.1016/j.tws.2011.05.010

**Do Nascimento J.W.B., Neto J.P.L., and Montross M.D., 2013.** Horizontal pressures in cylindrical metal silos and comparison with different international standards. Eng. Agric., 33(4), 601-611, https://doi.org/10.1590/S0100-69162013000400002

**Drucker D.C. and Prager W., 1952.** Soil mechanics and plastic analysis or limit design. Q. Appl. Math., 10(1), 157-165, https://doi.org/10.1090/qam/48291

**EN 1991-4, 2006,** Actions on structures. Part 4: Silos and tanks, European Commitee for Standardization, Brussels, Belgium.

**Gallego E., Rombach G.A., Neumann F., and Ayuga F., 2010.** Simulations of granular flow in silos with different finite element programs: ANSYS vs. SILO. Trans. ASABE., 53(3), 819-829, https://doi.org/10.13031/2013.30065

**Guaita M., Couto A., and Ayuga F., 2003.** Numerical simulation of wall pressure during discharge of granular material from cylindrical silos with eccentric hoppers. Biosyst. Eng., 85(1), 101-109, https://doi.org/10.1016/S1537-5110(03)00037-0

**Kibar H., 2017.** Patterns between wall pressures and stresses with grain moisture on cylindrical silo. Struct. Eng. Mech., 62(4), 487-496, https://doi.org/10.12989/sem.2017.62.4.487

**Kibar H. and Ozturk T., 2014.** The evaluation with ANSYS of stresses in hazelnut silos using Eurocode 1. Struct. Eng. Mech., 51(1), 15-37, https://doi.org/10.12989/sem.2014.51.1.015

**Keiter T.W.R. and Rombach G.A., 2001.** Numerical aspects of FE simulations of granular flow in silos. J. Eng. Mech., 127(10), 1044-1050, https://doi.org/10.1061/(ASCE)0733-9399(2001)127:10(1044)

**Kumar R., Patel C.M., Jana A.K., and Gopireddy S.R., 2018.** Prediction of hopper discharge rate using combined discrete element method and artificial neural network. Adv. Powder Technol., 29(11), 2822-2834, https://doi.org/10.1016/j.apt.2018.08.002.

**Matchett A.J., O'Neill J.A., and Shaw P., 2009.** Stresses in bulk solids in wedge hoppers: A flexible formulation of the coordinate specific, Lame-Maxwell equations for circular arc, principal stress systems. Powder Technol., 194 (3), 166-180, https://doi.org/10.1016/j.powtec.2009.04.002

**Michalowski R.L., 1983.** Approximate theory of loads in plane asymmetrical converging hoppers. Powder Technol., 36(1), 5-11, https://doi.org/10.1016/0032-5910(83)80002-3

**Molenda M., Montross M.D., Thompson S.A., and Horabik J., 2009.** Asymmetry of model bin wall loads and lateral pressure induced from two- and three-dimensional obstructions attached to the wall. Trans. ASABE., 52(1), 225-233, https://doi.org/10.13031/2013.25942

**Moya M., Aguado P.J., and Ayuga F., 2013.** Mechanical properties of some granular agricultural materials used in silo design. Int. Agrophys., 27(2), 181-193, https://doi.org/10.2478/v10247-012-0084-9

**Moya M., Ayuga F., Guaita M., and Aguado P., 2002.** Mechanical properties of granular agricultural materials. Trans. Am. Soc. Agric. Eng., 45(5), 1569-1577, https://doi.org/10.13031/2013.11062

**Munch-Andersen J., Askegaard V., and Brink A., 1992.** Silo model tests with sand. Bull. Danish Build. Res. Inst. 91.

**Ramírez A., Nielsen J., and Ayuga F., 2010.** Pressure measurements in steel silos with eccentric hoppers. Powder Technol., 201(1), 7-20, https://doi.org/10.1016/j.powtec.2010.02.027

**Rotter J.M., 2001.** Guide for the economic design of circular metal silos. CRC Press, London, UK, https://doi.org/10.4324/9780203477816

**Rotter J.M., 2009.** Silo and hopper design for strength, in: Bulk Solids Handl. Equip. Sel. Oper., Wiley, https://doi.org/10.1002/9781444305449.ch3

**Rotter J.M., Goodey R.J., and Brown C.J., 2019.** Towards design rules for rectangular silo filling pressures. Eng. Struct., 198(1), 109547, https://doi.org/10.1016/j.engstruct.2019.109547

**Vidal P., Gallego E., Guaita M., and Ayuga F., 2008.** Finite element analysis under different boundary conditions of the filling of cylindrical steel silos having an eccentric hopper. J. Constr. Steel Res., 64(4), 480-492, https://doi.org/10.1016/j.jcsr.2007.08.005

**Vidal P., Gallego E., Guaita M., and Ayuga F., 2006a.** Simulation of the filling pressures of cylindrical steel silos with concentric and eccentric hoppers using 3-dimensional finite element models. Trans. ASABE., 49(6), 1881-1895, https://doi.org/10.13031/2013.22290

**Vidal P., Couto A., Ayuga F., and Guaita M., 2006b.** Influence of hopper eccentricity on discharge of cylindrical mass flow silos with rigid walls. J. Eng. Mech.-ASCE., 132 (9), 1026-1033, https://doi.org/10.1061/(ASCE)0733-9399(2006)132:9(1026)

**Walker D.M., 1966.** An approximate theory for pressures and arching in hoppers. Chem. Eng. Sci., 21(11), 975-997, https://doi.org/10.1016/0009-2509(66)85095-9

**Wang Y., Lu Y., and Ooi J.Y., 2013.** Numerical modelling of dynamic pressure and flow in hopper discharge using the Arbitrary Lagrangian-Eulerian formulation. Eng. Struct. 56(1), 1308-1320, https://doi.org/10.1016/j.engstruct.2013.07.006

**Xiao H., Fan Y., Jacob KV., Umbanhowar P.B., Kodam M., Koch J.F., and Lueptow R.M., 2019.** Continuum modelling of granular segregation during hopper discharge. Chem. Eng. Sci., 193(1), 188-204, https://doi.org/10.1016/j.ces.2018.08.039

**Zhang Y., Jia F., Zeng Y., Han Y., and Xiao Y., 2018.** DEM study in the critical height of flow mechanism transition in a conical silo. Powder Technol., 331(1), 98-106, https://doi.org/10.1016/j.powtec.2018.03.024

**Zheng Q.J. and Yu A.B., 2015.** Finite element investigation of the flow and stress patterns in conical hopper during discharge. Chem. Eng. Sci., 129(1), 49-57, https://doi.org/10.1016/j.ces.2015.02.022

**Zheng Q.J., Xia B.S., Pan R.H., and Yu A.B., 2017.** Prediction of mass discharge rate in conical hoppers using elastoplastic model. Powder Technol., 307(1), 63-72, https://doi.org/10.1016/j.powtec.2016.11.037